J. Cell. Mol. Med. Vol 12, No 6B, 2008 pp. 2704-2716

Acrolein: unwanted side product or contribution to antiangiogenic properties of metronomic cyclophosphamide therapy?

M. Günther, E. Wagner, M. Ogris *

Pharmaceutical Biology-Biotechnology, Department of Pharmacy, Ludwig-Maximilians-Universität, Butenandtstr, Munich, Germany

Received: September 4, 2007; Accepted: January 23, 2008

Abstract

Tumour therapy with cyclophosphamide (CPA), an alkylating chemotherapeutic agent, has been associated with reduced tumour blood supply and antiangiogenic effects when applied in a continuous, low-dose metronomic schedule. Compared to conventional high-dose scheduling, metronomic CPA therapy exhibits antitumoural activity with reduced side effects. We have studied potential antiangiogenic properties of acrolein which is released from CPA after hydroxylation. Acrolein adducts were found in tumour cells and tumour endothelial cells of CPA-treated mice, suggesting an *in vivo* relevance of acrolein. *In vitro*, acrolein inhibited endothelial cell proliferation, endothelial cell migration and tube formation. Moreover, acrolein caused disassembly of the F-actin cytoskeleton and inhibition of $\alpha v\beta 3$ integrin clustering at focal adhesions points in endothelial cells. Acrolein treatment modulated expression of thrombospondin-1 (TSP-1), an endogenous inhibitor of angiogenesis known to be linked to antiangiogenic effects of metronomic CPA therapy. Further on, acrolein treatment of primary endothelial cells modified NF-κB activity levels. This is the first study that points at an antiangiogenic activity of acrolein in metronomically scheduled CPA therapy.

Keywords: cyclophosphamide • metronomic • angiogenesis • acrolein

Introduction

Cyclophosphamide (CPA) is a well-known chemotherapeutic agent being applied for a broad range of malignant diseases. After activation by hydroxylation through the liver cytochrome system the drug is released into the blood stream and decomposes to DNA cross-linking phosphoramide mustard and acrolein which causes DNA cross-links [1] and protein denaturation [2]. In conventional treatment regimes the phosphoramide mustard is considered to mediate antitumoural activity, whereas acrolein is recognized as a side product responsible for unwanted toxic effects [3]. Besides the classical high-dose bolus therapy a different application scheme is also used in the clinic: moderate, frequent doses of CPA are applied, resulting in reduced toxic side effects but sustained antitumoural activity (metronomic schedule) [4, 5]. In these metronomic scheduled treatment regimes, antitumoural effects are associated with decreased angiogenesis resulting in reduced intratumoural microvascular density [6].

Since it was discovered that metronomic CPA therapy not only causes cytotoxic activity on tumour cells but also affects tumour endothelial cells and modulates antiangiogenic cytokine expression, research has focused on the mechanism of such antiangiogenic treatment regimes. Activated CPA was shown to inhibit endothelial cell proliferation and endothelial cell migration *in vitro*; metronomic CPA treatment regimes lead to apoptosis of endothelial cells in tumour blood vessels [5] and to reduction in tumour blood flow [7]. In this context, induction of endogenous thrombospondin-1 (TSP-1) expression, an antiangiogenic cytokine, was suggested as a key mediator of antiangiogenic effects in the tumour microenvironment induced by low-dose metronomic scheduling of CPA [8, 9]. *In vitro*, TSP-1 led to profound reduction in endothelial proliferation, migration and differentiation capability and induced apoptosis in endothelial cells [10, 11].

*Correspondence to: Manfred OGRIS,
Pharmaceutical Biology-Biotechnology
Ludwig-Maximilians-Universität, Butenandtstr. 5-13
D-81377 Munich, Germany.
Tel.: +49 89 21 80 77 84 2
Fax: +49 89 21 80 77 79 1
E-mail: Manfred.Ogris@cup.uni-muenchen.de

doi:10.1111/j.1582-4934.2008.00255.x

However, despite the intensive investigation on metronomic CPA therapy the role of single CPA metabolites, which may mediate antiangiogenic effects, has not been clarified yet. DeLeve and colleagues [12] and also Kachel *et al.* [13] tried to distinguish cytotoxic effects mediated either by acrolein or phosphoramide mustard on *in vitro* cultures of endothelial cells. Incubation with 4-Hydroperoxy-CPA (4-OOH-CPA) resulted in dose-dependent cytotoxic effects in endothelial cells, however, with acrolein alone also a dose-dependent toxicity was described. Further studies indicated that acrolein is transported *via* the blood stream to peripheral sites *in vivo* [13, 14]. Acrolein also interacts with the F-actin cytoskeleton [15] leading to depolymerization and inhibition of migration in fibroblasts and inhibits cell attachment in a dose-dependent manner [16]. Further on, acrolein was described to interact with NF-κB-regulated gene expression at sublethal doses in lung adenocarcinoma cells [17] and epithelial cells [18] and alkylates cysteine and arginine residues of the NF-κB1-binding domain [19]. NF-κB is involved in the expression of several growth-related cytokines and in mediation of cell proliferation, survival [20] and the angiogenic phenotype of endothelial cells [21].

The angiogenic process is driven by a complex co-action between tumour cells, stroma cells and endothelial cells including several proangiogenic and antiangiogenic factors [22]. Thus, the angiogenic process provides several targets to intervene and to ultimately reduce tumour growth by disturbing the neoangiogenic process. Nevertheless, there is no clear evidence how acrolein influences neovascularization in growing solid tumours. In this study we characterized the antiangiogenic effects of acrolein on tumours and the mechanism lying behind its antiangiogenic activity towards endothelial cells. Acrolein adducts were found in tumour tissue both within tumour cells and endothelial cells. We were able to show that acrolein negatively affects proliferation, migration and differentiation of endothelial cells. Acrolein disturbed endothelial F-actin polymerization and integrin $\alpha v\beta 3$ receptor clustering at focal adhesion points. A concentration-dependent effect of acrolein was found regarding activity levels of NF-κB and expression profile of TSP-1.

Materials and methods

Reagents and chemicals

Cell culture medium and foetal bovine serum (FBS) were purchased from Invitrogen GmbH (Karlsruhe, Germany). Linear polyethylenimine (LPEI) was synthesized by acid-catalysed deprotection of poly(2-ethyl-2-oxazoline) (50 kD, Aldrich) in analogous form as described [23] and is commercially available from Polyplus (Straßbourg, France). Plasmid pNF-κB-LUC (Luciferase under control of a NF-κB sensitive promoter/enhancer) was obtained from Clontech Laboratories, Inc. (Mountain View, CA, USA), plasmid pCMV-LUC (Photinus pyralis luciferase under the control of the CMV promoter/enhancer) is described in Ref. [24]. Plasmids were purified with the EndoFree Plasmid Kit from Quiagen GmbH (Hilden, Germany).

The antibody for detection of NF-κB p105/50 was purchased from Cell Signaling Technology, Inc. (Danvers, MA, USA), NF-κB p65 antibody (clone sc372) was obtained from Santa Cruz Biotechnology (Santa Cruz, CA, USA). Peroxidase labelled anti-rabbit and anti-mouse antibodies for Western blot analysis were purchased from Vector Laboratories (Peterborough, England). The antibody for detection of protein bound acrolein was obtained from JaICA (Fukuroi, Japan), mouse-anti-human CD51/CD61 and IgG1 isotype control were obtained from Dako (Copenhagen, Denmark). Rat-anti-mouse CD31 antibody was purchased from CALTAG (Burlingame, USA); Alexa labelled secondary antibodies were obtained from Invitrogen (Karlsruhe, Germany). Vectashield-mounting medium for fluorescence microscopy was obtained from Vector laboratories INC (Burlingame, CA, USA), TSP-1 competitive ELISA (ChemiKine, Human TSP-1 EIA KIT) was from Chemicon (Temecula, CA, USA). Protein content was determined by the BCA Protein Assay KIT (Pierce, Rockford, IL, USA). 4-OOH-CPA was obtained from Dr Ulf Niemeyer, Niomech IIT GmbH (Bielefeld, Germany). All other regents were purchased from Sigma-Aldrich (Munich, Germany).

Primary cells and cell lines

HUVEC cells were obtained from Cambrex Bio Science (Verviers, Belgium) and used between passage 3 and 7. Cells were grown on collagen G coated flasks in M199 medium supplemented with 10% FBS, 10 ng/ml human bFGF and antibiotics. Porcine endothelial cells (PEC) cells were isolated asdescribed recently [25] and grown on collagen G coated flasks in M199 medium supplemented with 10% FBS and antibiotics. CT26 tumour cells (ATCC CRL-2638) were grown in Dulbecco's Modified Eagle's Medium (DMEM) medium supplemented with 10% FBS and antibiotics. Prior to tumour transplantation cells were grown for three passages in antibiotic free medium. All cultured cells were grown at 37°C in 5% CO_2 humidified atmosphere.

Measurement of acrolein concentrations in cell culture medium

To monitor maximum concentrations of unbound acrolein in serum containing medium (acrolein peak concentration), measurements were performed in a separate experiment using sealed tubes. Detection of acrolein was carried out in the supernatant after protein precipitation as recently described [26]. With different concentrations of acrolein added to serum-containing medium, free acrolein was detected either directly after adding acrolein or after 0.5 hr, 1.5 hrs or 48 hrs of incubation at 37°C. In brief, protein was precipitated after addition of 100 µl 0.015 N HCl, 200 µl of a ZnSO4 (5% w/v) solution and 200 µl of a $Ba(OH)_2$ (2.5% w/v) solution to 500 µl of medium with 10% FBS (v/v) and known acrolein concentrations at room temperature. The precipitate was removed by centrifugation and free acrolein was detected in the supernatant after derivatization with 3-aminophenol at 90°C for 25 min. Fluorescence measurements were carried out at room temperature with an excitation wavelength of 346 nm and emission wavelength of 514 nm, respectively, using a Cary Eclipse fluorimeter (Cary, Mulgrave, Australia). As a control, similar measurements were carried out with serum free medium. Maximum acrolein concentrations were measured immediately after addition of acrolein and are shown in the respective figures (measured acrolein peak concentration).

Measurement of NF-κB activity

Measurement of NF-κB activity in HUVEC and CT26 tumour cells was performed in the absence or presence of indicated acrolein concentrations in the medium. CT26 tumour cells were seeded on 24-well plates at a density of 15,000 cells/well 24 hrs prior to transfection. HUVEC cells were seeded on collagen coated (Collagen G, Biochrom) 24-well plates at a density of 15,000 cells/well 24 hrs prior to transfection. Transfection with LPEI (300 ng DNA/well, as described in [27] was carried out either with pNF-κB-LUC or pCMV-LUC plasmid. Twenty-four hours after transfection, indicated amounts of acrolein (dissolved in Phosphate Buffered Saline (PBS)) were added to the cells. After further cultivation for 24 hrs luciferase activity was quantified and protein content was determined by the BCA Protein Assay KIT according to manufacturers protocol. NF-κB induced luciferase expression was normalized to pCMV-LUC expression and protein content.

Western blot analysis

Western blot analysis was performed as previously described loading equal amounts of total protein per lane [28]. Briefly, the blot was probed with a monoclonal antibody raised against NF-κB p105/p50 (1:1000, Cell Signaling Biotechnology) or NF-κB p65 (1:1000, Santa Cruz Biotechnology) at 4°C overnight. Membranes were then exposed to a peroxidase labelled anti-rabbit secondary antibody (1:5000, Vector Laboratories) followed by a luminescence detection of antibody binding (ECL, Amersham Biosciences, Buckinghamshire, UK).

Tumour transplantation and drug administration

Female and male Severe Combined Immunodeficiency Disorder (SCID) mice (CB17/Icr-PrkdcSCID/Crl) aged 8–10 weeks were housed in individually vented cages under specific pathogen free conditions with a 12 hrs day/night cycle and with food and water ad libitum. CT26 cells were cultivated as described and harvested when reaching approx. 70–80% confluence. After washing with PBS 10^5 tumour cells in 100 µl PBS were injected subcutaneously. As soon as tumours were visible (approx. 1 mm in one dimension), tumour growth was measured with a caliper. Each measurement consisted of three diameters each 90° apart and tumour volume was calculated by the formula a*b*c*0.4 (with a, b and c indicating the three diameters). The vehicle group (PBS) and the drug treatment group (CPA dissolved in PBS) were housed separately. Treatment was started when tumour reached an average volume of 40 mm^3 (11 days after tumour inoculation) and was continued until the end of the experiment. The vehicle solution (PBS) and the drug solution was administered intraperitoneally. The mice obtained drug treatment on two consecutive days followed by intermission of 2 days. All animal procedures were approved and controlled by the local ethics committee and carried out according to the guidelines of the German law for protection of animal life.

Vascular fluorescent perfusion

Hoechst 33258 was used as a marker for blood perfused areas in the tumour. Five minutes after intravenous injection of 200 µl Hoechst 33258 in PBS (2.5 mg/ml) mice were sacrificed, tumours resected, embedded in OTC medium and immediately frozen. Assessments were made either at the end of the experiment (day 28 after tumour setting) or when tumour size exceeded 15 mm in one dimension. Cryosections (10 µm) were cut on a cryostat at three different regions, starting at the tumour periphery towards the equatorial plate. Sections were viewed with an Axiovert 200 inverted microscope (Zeiss, Jena, Germany) equipped with appropriate excitation (365 nm) and emission (420 nm long pass) filters and a 5 × 0.12 NA objective (Carl Zeiss, Jena, Germany). Nine sections per tumour were examined and five fields per section were randomly selected for image analysis. Hoechst 33258 fluorescence was quantified by image analysis using MIPAV software (Medical Image Processing, Analysis and Visualization). The software can be downloaded at http://mipav.cit.nih.gov/.

Cell viability

HUVEC and PEC were plated in complete medium in a collagen G coated 24-well plate at 15,000 cells per well and incubated over night. Acrolein, dissolved in PBS, was added to the cells at indicated concentrations. After 1 or 3 days of incubation with acrolein, metabolic activity of cells was quantified by MTT assay as recently described [29].

Scratch wound assay

HUVEC and PEC cells were plated onto collagen G coated glass cover slips (15,000 cells/well) 24 hrs prior performing the scratch wound assay. The confluent monolayer was scratched by a pipette tip, rinsed with PBS to remove detached cells and fresh medium was added. Digital images of cells were taken immediately after scratching (t = 0) or after the indicated incubation time either in the presence or absence of acrolein. The distance between cells in the scratched area was measured using the Axio vision LE software (Zeiss, Jena, Germany). Ten measurements were performed for each data point. Results were normalized to untreated control cells.

Tube formation assay

Cooled matrigel (Sigma, Munich, Germany) was added to each well (96-well plate: 50 µl, 24-well plate: 300 µl per well, respectively) and incubated at 37°C for 30 min to allow solidification. HUVEC cells were harvested at a density of 70% confluence. Tube formation assay was performed as described [30]. Cells were incubated for 4 hrs in the absence or presence of indicated concentrations or acrolein. Cells were fixed with 4% paraformaldehyde (in PBS) and total amount of tube-like structures without intersections were analysed *via* transmitted light microscopy.

Immunohistochemistry

HUVEC cells were cultured on collagen G coated Lab-Tek slides (Nunc, Rochester, New York, USA) and treated with indicated concentrations of acrolein. Thereafter, cells were washed with PBS, fixed with 4% paraformaldehyde in PBS and permeabilized with 0.1% Triton-X 100 in PBS. After blocking with 0.5% FBS in PBS cells were stained with mouse-anti-human CD51/61 (Dako, Copenhagen, Denmark) and Cy5 labelled anti-mouse antibody (Jackson, ImmunoResearch Laboratories, Inc., West Baltimore Pike, USA). Actin fibres were stained with Phalloidin-FITC (Sigma) at a final concentration of 0.165 µM; after washing with PBS and embedding in mounting medium (Vector Labs, Burlingame, CA, USA) cells

were viewed on a Zeiss Axiovert 200 microscope using appropriate filter sets for FITC and Cy5.

Cryosections (5 µm) of CT26 tumours were fixed, permeabilized and blocked as described above. Acrolein adducts were stained with a monoclonal mouse antibody directed against acrolein-protein adducts and Alexa-488 goat anti-mouse. Control antibody staining was performed with mouse IgG1 control antibody. Tumour endothelial cells were stained with rat-anti-mouse-CD31 antibody and Alexa-647 goat anti-rat antibody.

Flow cytometric analysis of integrin αvβ3 receptor on HUVEC cells

HUVEC cells grown on collagen G coated 24-well plates (TPP, Switzerland) were harvested with collagenase and stained on ice for integrins αvβ3 (mouse-anti-human CD51/61 followed by Alexa-488 goat antimouse). Control staining was performed using irrelevant control antibodies. Cells were analysed on a Cyan™ MLE flow cytometer (Dako) using 488 nm laser excitation, emission was detected by using a 530/40 nm bandpass filter. Data analysis was performed as described recently [31].

Thrombospondin ELISA

HUVEC cells were seeded on collagen G coated 24-well plates at a density of 15,000 cells per well. 24 hrs after seeding, cells were treated with indicated concentrations of acrolein in medium for further 24 hrs. After treatment, cells were washed with PBS followed by cell lysis with 100 µl distilled water and a freeze-thaw cycle. After centrifugation (16,000 g, 60 min, 4°C) 25 µl supernatant was diluted with Diluent no.2 (ChemiKine, Human TSP-1 EIA KIT, Chemicon, USA) to a total volume of 100 µl and analysed for TSP-1 level by the ChemiKine Human TSP-1 EIA KIT according to manufacturers protocol. TSP expression was normalized to protein content. Experiments were carried out in duplicates.

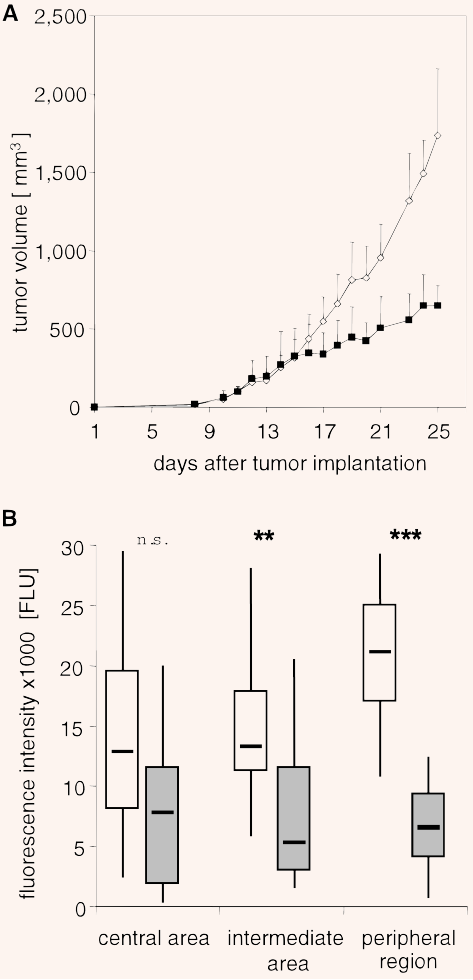

Fig. 1 Metronomic cyclophosphamide (CPA) treatment of CT26 tumours. (**A**) Tumour growth delay by metronomically scheduled intraperitoneal application of CPA (40 mg/kg on two consecutive days followed by 2 days without treatment) in a subcutaneous CT26 tumour model. Treatment started at an average tumour volume of 40 mm^3. Open symbols: control animals; full symbols: CPA-treated animals. Mean tumour volumes (±SD) are shown for each treatment group; (n = 10 in each group). (**B**) SCID mice bearing subcutaneous CT26 tumours were treated with metronomically scheduled CPA as indicated; intravenous injected Hoechst 33258 stain was used as a tracer for functional vasculature. After resection, tumours were cryosectioned and Hoechst 33258 fluorescence signal was quantified. From each tumour 3 × 3 sections of the indicated tumour region (central area, intermediate area and tumour peripheral region) were analysed. Open symbols: control tumours; filled symbols: CPA-treated tumours. Medians were determined from slides of six animals in the control group and 10 animals in the CPA-treated group, including lower quartile, upper quartile as well as smallest and largest observation. n.s. = not significant, $***P < 0.001$; $**P < 0.01$ compared to control tumours (Mann–Whitney U-test).

Results

Metronomic CPA treatment of CT-26 murine colon carcinoma tumours results in decreased tumour blood supply and acrolein adducts in the tumour tissue

SCID mice bearing subcutaneously implanted CT26 murine colon adenocarcinoma tumours were treated with metronomically scheduled CPA (40 mg/kg on two consecutive days followed by 2 days without treatment) starting 11 days after tumour implantation. A significantly reduced tumour growth was observed from day 19 on and the calculated tumour volume doubling time increased 2.5-fold compared to control animals (Fig. 1A). Treatment was well tolerated and no significant decrease in bodyweight was observed (data not shown). To follow possible antiangiogenic effects resulting from the metronomic treatment regime, we analysed the tumour blood flow by using Hoechst 33258 dye

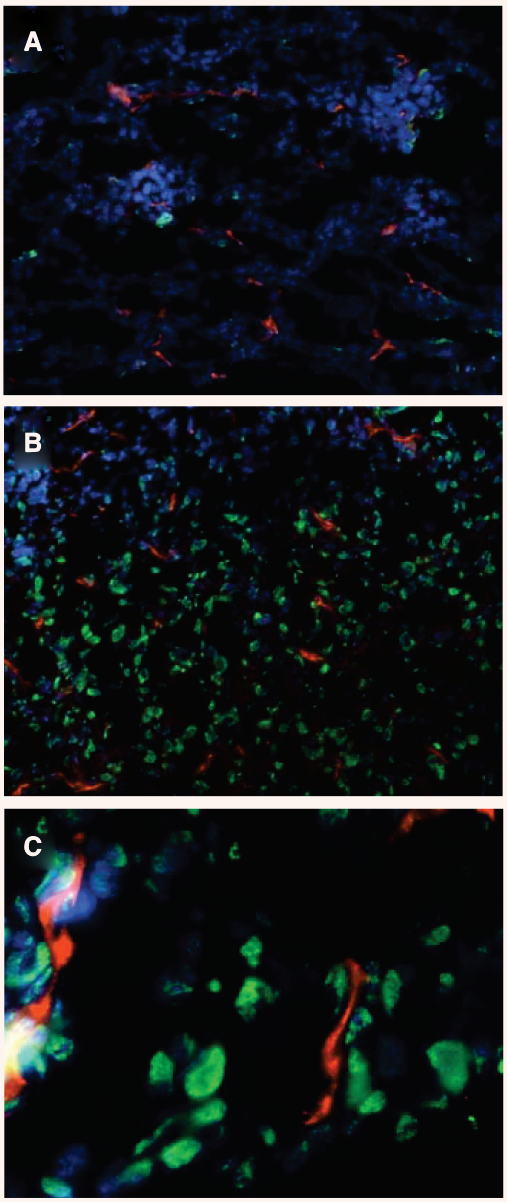

Fig. 2 Acrolein adducts in CT26 tumours. Cryosections (5 μm) were stained with specific antibodies for endothelial cells (rat-anti-mouse CD31 (red)) and acrolein modified proteins (green). Cell nuclei are stained by intravenously applicated Hoechst 33258 dye (blue). Untreated control tumour (**A**); CPA-treated tumour (**B**) and (**C**). Fluorescence microscopy of stained cryosections was carried out using an Axiovert 200 fluorescence microscope equipped with a Zeiss Axiocam camera. Light was collected through a 20 × 0.4 NA (**A, B**) or 63 × 1.4 oil immersion objective (**C**).

as a tracer. After systemic application of Hoechst dye mice were sacrificed, tumours resected and the relative Hoechst fluorescence was measured in the cryosections of tumour tissue (Fig. 1B). Tumours sections were subdivided into a peripheral region, an intermediate and a central area and the fluorescence signal was quantified within the distinct regions. Metronomic CPA treatment resulted in significantly decreased blood supply in the intermediate and peripheral areas of the tumours. Reduction in fluorescence signal was most pronounced in the peripheral region of the tumour, indicating reduced blood flow and antiangiogenic effects (Fig. 1B). We also observed a reduced vessel density after CPA treatment when staining for the endothelial cell marker CD31 (data not shown). To evaluate a possible contribution of the metabolite acrolein to the effects of metronomically scheduled CPA, tumour sections were stained with an antibody directed against acrolein-protein adducts. Acrolein adducts were detected both in tumour cells and endothelial cells of CPA treated tumours (Fig. 2). Acrolein-protein adducts in the tumour indicate accessibility of tumour tissue and tumour vessels to acrolein and supports a possible role of this metabolite *in vivo*. It is noteworthy that acrolein adducts were often detected in tumour areas with low blood supply, indicated by low-Hoechst33258 fluorescence signal.

Detection of acrolein concentrations in cell culture medium

The α,β-unsatured aldehyde acrolein is a highly reactive compound, resulting in fast decrease of free acrolein in serum-containing medium. Therefore, monitoring of unbound acrolein is crucial for correct evaluation of active acrolein concentrations in cell culture experiments. When quantifying free acrolein in the presence of serum, maximum concentrations of acrolein were detected directly after addition of acrolein to FBS containing medium (35% of added acrolein = acrolein peak concentration). After 30 min of incubation in serum-containing medium only 25% of total acrolein was detected in free form, whereas in the absence of serum the recovery rate was almost 100%. The acrolein concentrations further decreased with incubation time. However, about 5% of added acrolein was detectable, even after 48 hrs of incubation in FBS containing medium.

Effects of acrolein on proliferation, migration and differentiation of endothelial cells and on proliferation of tumour cells

We have compared the antiproliferative effect of acrolein and 4-OOH-CPA on primary human endothelial cells (HUVEC) (Fig. 3A). Four-hydroperoxy-CPA is rapidly converted to 4-OH-CPA in aqueous solution and can be considered equivalent to 4-OOH-CPA under experimental conditions [32]. Incubation with 4-OOH-CPA significantly reduced HUVEC proliferation at 30 and 50 μM after a 3 day treatment, but also acrolein alone inhibited the proliferation

of HUVEC to a similar extent. The reduction in proliferation of endothelial cells indicates the importance of the metabolite acrolein in the context of the angiogenic process.

For evaluation of acute toxic effects of acrolein, survival of primary endothelial cells (PECs and HUVECs) was determined 24 hrs after the administration of acrolein to the culture medium. Decrease in metabolic activity resulting from the acrolein treatment was more pronounced in PEC compared to HUVEC cells (Fig. 3B). At 25 μM acrolein (added) metabolic activity of PEC cells was decreased to 10%, whereas for HUVEC a concentration of >50 μM (added) was necessary to achieve a similar effect.

Antiproliferative effects of acrolein were also evident on CT26 tumour cells in a dose- dependent manner. Culturing CT26 cells in the presence of 30 μM acrolein (added) in the medium resulted in reduction of metabolic activity to 70% and to 50% at 40 μM (added) compared to untreated cells (Fig. 3C).

Besides proliferation, migration capability of endothelial cells is crucial for the angiogenic process. The potential of endothelial cells to migrate in monolayer culture was estimated in the scratch-wound assay. Migration capability of HUVEC cells was decreased by over 50% in the presence of 20 μM acrolein (added) and by 80% with 25 μM acrolein (added) (Fig. 4A); a concentration of 15 μM acrolein (added) decreased migration of PEC by 80% compared to untreated control cells (Fig. 4B).

Another important feature of endothelial cells in the process of neovascularization is the ability to form tube-like structures. Tube formation was assessed with HUVEC on matrigel. When HUVEC were subcultured on matrigel in vehicle-treated experiments, tube formation was achieved within 4 hrs. In the presence of acrolein, tube formation was inhibited in a concentration-dependent manner (Fig. 4C). Even 10 μM acrolein (added) exhibited a marked effect on tube formation visible by the disruption of these structures; the number of tubes without intersections decreased by approx. 70%. Performing the matrigel assay in the presence of 30 μM acrolein (added) resulted in nearly complete inhibition of tube formation. Applied acrolein concentrations did not interfere with the viability of endothelial cells within the observation period (compare Fig. 3B), indicating that acrolein inhibited migration and differentiation of primary endothelial cells in a sublethal concentration range.

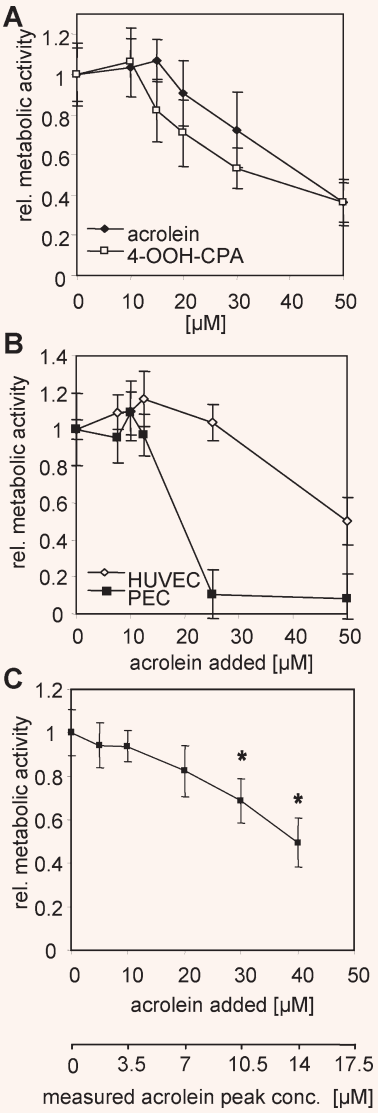

Fig. 3 Influence of acrolein on survival of tumour cells and endothelial cells. Cell survival was determined by measuring metabolic activity with the MTT assay. Values are normalized to metabolic activity of untreated control cells. The upper x-axis in **A–C** indicates the concentration of total acrolein (and 4-OOH-CPA in **A**) added; the second x-axis at the bottom of the figure reflects the concentrations of free acrolein measured in the cell culture medium used immediately after addition of acrolein (acrolein peak concentration) as described in materials and methods. (**A**) Metabolic activity of primary endothelial cells (HUVECs) treated with indicated concentrations of 4-OOH-CPA (open symbols) or acrolein (full symbols) after a 3 day treatment period (mean ± SD for $n = 3$ replicates). (**B**) Metabolic activity of primary endothelial cells treated with indicated concentrations of acrolein for 24 hrs. Cell survival of HUVECs (open symbols) and PEC cells (full symbols) was determined (mean ± SD for $n = 3$ replicates). (**C**) Metabolic activity of CT26 tumour cells treated with indicated concentrations of acrolein for 24 hrs (mean ± SD for $n = 4$ replicates).

Acrolein influences F-actin cytoskeleton and integrin αvβ3 clustering

To understand possible mechanisms underlying acrolein inhibition of migration and differentiation, changes in the F-actin cytoskeleton and integrin αvβ3 receptor clustering were investigated. Motility of endothelial cells largely depends on the F-actin cytoskeleton. In the presence of 10% FBS and 10 ng/ml bFGF, F-actin filaments of HUVEC were organized in stress fibres with some of them spanning across the entire cytoplasm (Fig. 5A). Incubation of proliferating HUVECs with sublethal concentrations of acrolein (10–20 μM, added acrolein) resulted in cytoskeletal

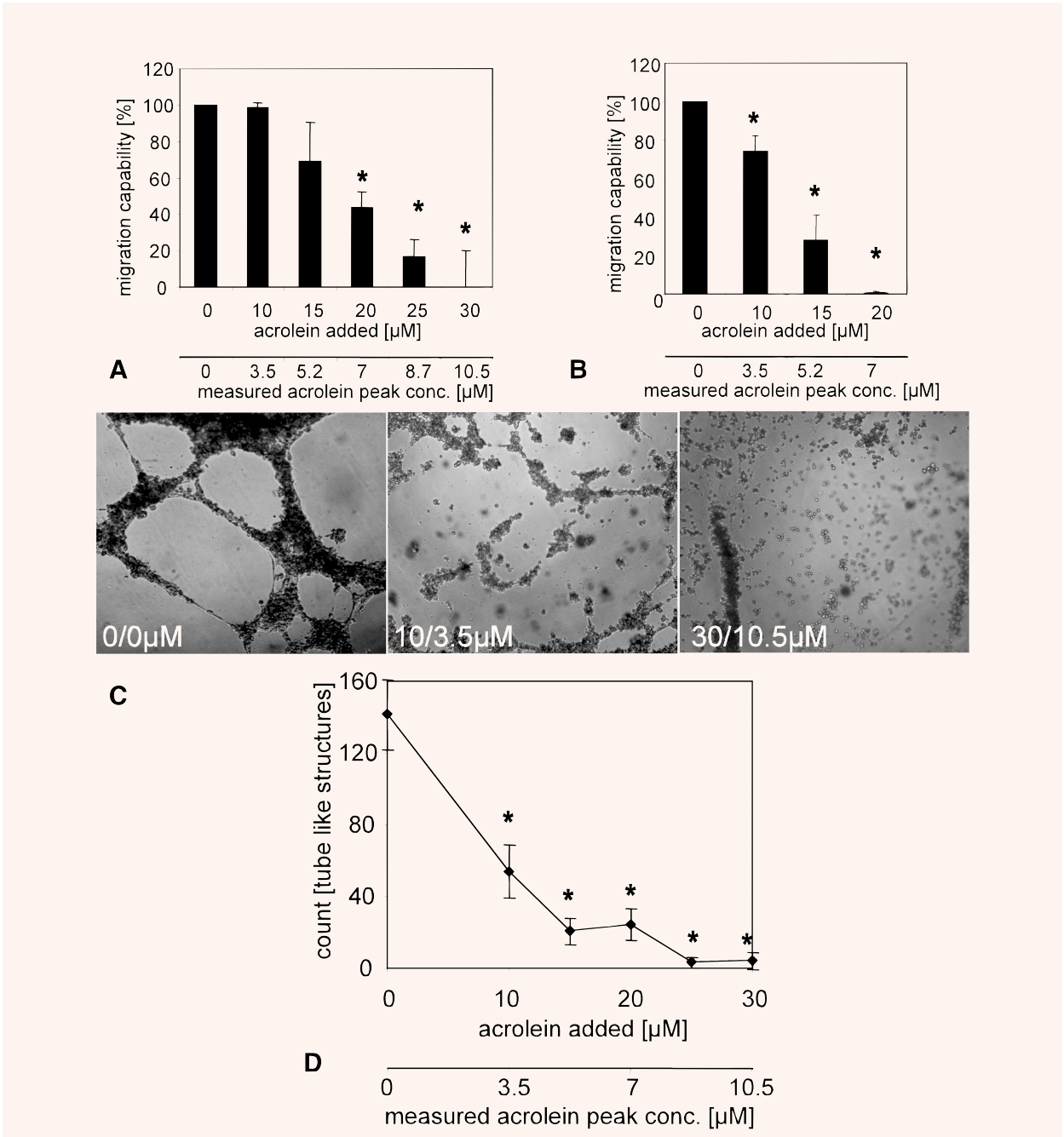

Fig. 4 Dose-dependent inhibition of migration (**A** and **B**) and tube formation (**C** and **D**) by acrolein in endothelial cells. The upper x-axis in **A**, **B** and **D** indicates the concentration of total acrolein added; the lower x-axis reflects the concentrations of free acrolein measured in the cell culture medium used immediately after addition of acrolein (acrolein peak concentration) as described in materials and methods. In **C**, total acrolein added is indicated by the first, acrolein peak concentration by the second number in the respective pictures. HUVEC (**A**) and PEC (**B**) were treated for 24 hrs with indicated concentrations of acrolein. A confluent cell layer of endothelial cells was scratched with a pipette tip and photographed. After 24 hrs

of incubation with increasing concentrations of acrolein cells were fixed and photographed again. In the absence of acrolein HUVEC cells as well as PEC cells grow again to a confluent monolayer and migration capability was set to 100%. Migration capability was normalized on migration of untreated control cells and is presented as mean ± SD for n = 10 replicates. $*P < 0.05$, compared to untreated control cells (Mann–Whitney U-test). (**C**) and (**D**): Dose-dependent inhibition of tube formation. HUVEC cells were treated in the matrigel tube formation assay in the absence or in the presence of indicated concentrations of acrolein for four hours. Transmission light microscopy was performed using an Axiovert 200 microscope equipped with a Sony DSC-S75 digital camera. Light was collected through a Zeiss 10 × 0.25 NA objective and images were captured using phase contrast (**C**). The number of tubes without intersections per field were counted 4 hrs after seeding. Three fields were counted for each data point. Mean values ± SD are shown for three values per datapoint (**D**). $*P < 0.05$, compared to untreated control cells (Mann-Whitney U-test).

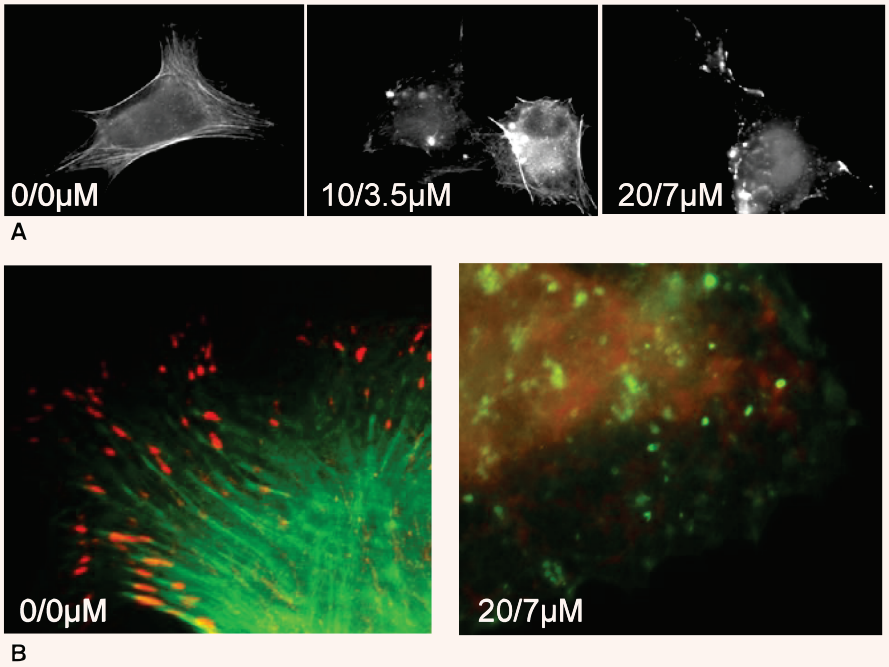

Fig. 5 Disruption of the HUVEC cytoskeleton by acrolein. HUVEC were cultured on a collagen G coated glass surface in the presence of 10% foetal bovine serum (FBS) and 10 ng/ml bFGF. Cells were treated with the indicated concentration of acrolein for 12 hrs and thereafter stained with phalloidin-FITC (**A**) or phalloidin-FITC (green) and anti- integrin αvβ3 (red) (**B**). Light was collected through a Zeiss 63 × 1.4 oil immersion objective. Total acrolein added is indicated by the first, acrolein peak concentration by the second number in the respective pictures.

disorganization and disruption of F-actin filaments within 12 hrs of incubation. Already at 10 μM acrolein (added), the F-actin fibres were partially depolymerized and the effect was even more pronounced at 20 μM (added). When removing acrolein from the supernatant, cells were able to remodel F-actin cytoskeleton to a certain degree within 24 hrs (data not shown). Incubation of HUVECs with 20 μM acrolein (added) for 12 hrs also led to dearrangement of integrin αvβ3 clustering (Fig. 5B) at focal adhesion points of the endothelial cells. The total amount of integrin αvβ3 receptor on the surface of the cells measured by flow cytometry remained unchanged (data not shown).

Modulation of endothelial NF-κB activity levels and endogenous TSP-1 expression

Further mechanistic investigations on the antiangiogenic effects of acrolein were performed in the context of modulation of endothelial NF-κB activity and TSP-1 expression.

Treatment of HUVEC cells with 10 μM and 20 μM acrolein (added) significantly decreased basal NF-κB activity within 24 hrs of treatment as detected by NF-κB sensitive reporter gene expression (Fig. 6A). NF-κB activity levels were reduced to 60% at 10 μM and to 40% at 20 μM acrolein (added) in the cell culture medium. Interestingly, NF-κB activity levels were found to be up-regulated when culturing was performed in the presence of 30 μM of acrolein (added). Levels of the precursor p105, NF-κB subunit p50 and NF-κB subunit p65 remained unchanged by acrolein treatment up to 20 μM acrolein (added) (Fig. 6B). Incubation of HUVEC cells with 30 μM of acrolein (added) resulted in significant decrease of the precursor p105 and the p50 subunit; levels of the p65 subunit remained unchanged, resulting in a modified ratio between p50 to p65 subunits.

In contrast to the regulations detected in endothelial cells, no influence of acrolein on NF-κB sensitive reporter gene expression was detected on CT26 tumour cells (data not shown).

Beneath NF-κB activity, TSP-1 levels were modulated by acrolein treatment in cultured primary HUVEC cells. Incubation of HUVECs

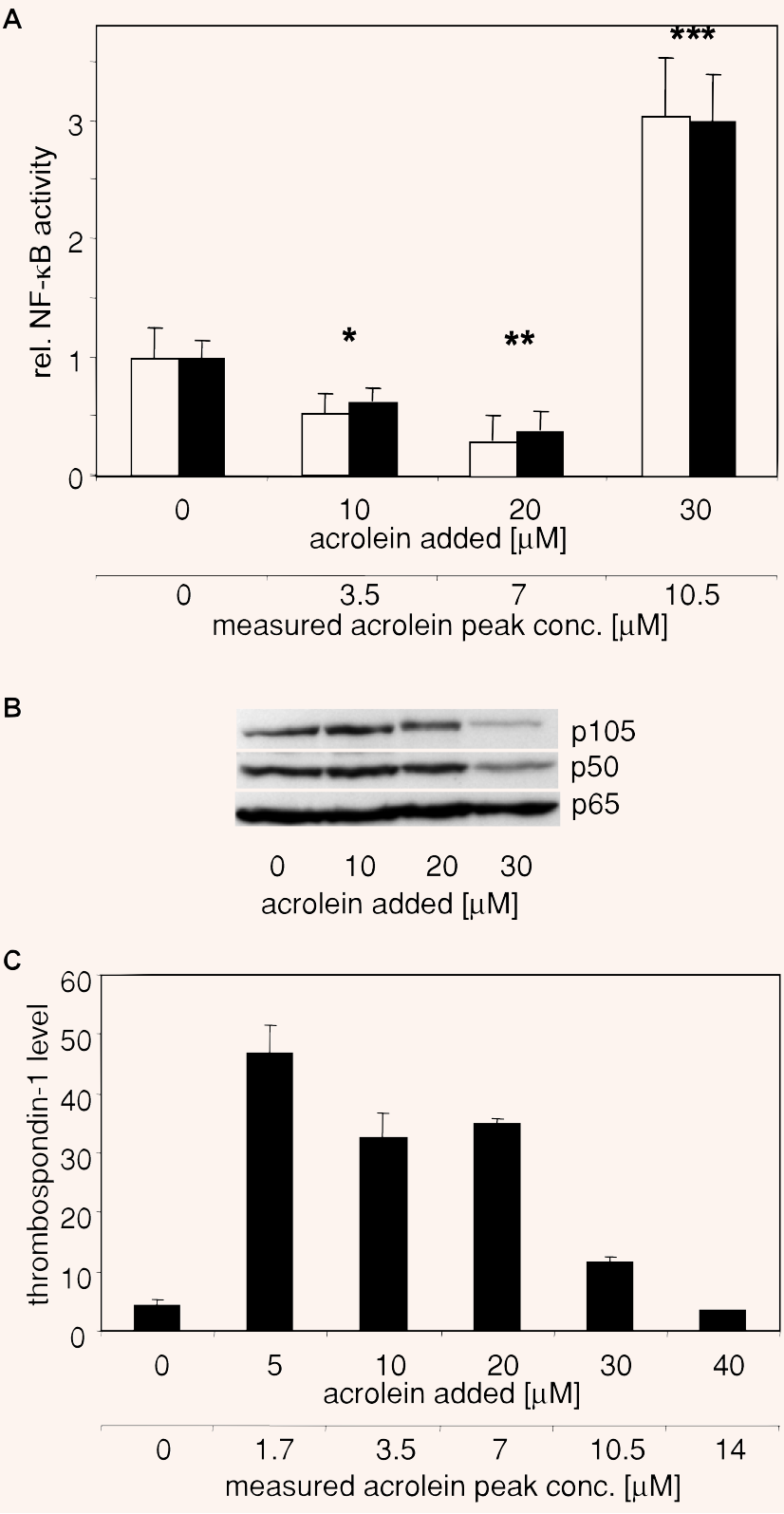

Fig. 6 Modulation of NF-κB activity and thrombospondin-1 expression in HUVEC cells by acrolein. In (**A**) and (**B**) the upper x-axis indicates the concentration of total acrolein added; the second x-axis at the bottom of the figure reflects the concentration of free acrolein measured in the cell culture medium used immediately after addition of acrolein (acrolein peak concentration) as described in materials and methods. (**A**) HUVEC cells were transfected with pNF-κB-LUC or the control plasmid pCMV-LUC. 24 hrs after transfection, cells were treated with indicated concentrations of acrolein for 24 hrs and luciferase activity measurement was performed thereafter; additionally, protein content was determined. Ratios of luciferase activity obtained with pNF-κB-LUC and pCMV-LUC (open columns) and relative luciferase activity obtained with pNF-κB-LUC in correlation to protein content (filled columns) are shown after normalization to untreated control cells. $n = 8 \pm$ SD, $^{*}P < 0.05$, $^{*}< 0.01$ and $^{***}P < 0.001$, compared to untreated cells (Mann-Whitney U-test). (**B**) HUVEC cells were cultivated in the presence of indicated concentrations of added acrolein for 24 hrs before analysis. Levels of NF-κB p105/50 and NF-κB p65 were measured by Western blot analysis. (**C**) HUVEC were cultured in the presence of indicated concentrations of acrolein for 24 hrs. Thrombospondin-1 was quantified in the cell lysates by competitive ELISA and normalized to total protein content.

with 5–20 μM acrolein (added) resulted in highly increased TSP-1 levels (up to 11-fold at 5 μM, added acrolein), whereas this effect was less pronounced at 30 μM (added) and above (Fig. 6C). The additionally performed protein content assay (BCA assay) exhibited unchanged total protein levels at all indicated concentrations.

Discussion

In the present work we studied the antiangiogenic activity of acrolein which is a metabolite of activated CPA [33]. Metronomic CPA treatment regimes have been linked to antiangiogenic effects and reduced microvessel density by affecting proliferation, survival and migration of endothelial cells and disturbance of angiogenic processes *in vivo* [5, 6]. Four-hydroxy-CPA (4-OH-CPA), the first metabolite of CPA after hydroxylation, is distributed systemically *via* the blood stream after activation by liver cytochrome P450. It exists in equilibrium with aldophosphamide which spontaneous releases phosphoramide mustard and acrolein [34]. Patients receiving CPA are exposed to measurable concentrations of acrolein: a CPA dose of 60 mg/kg body weight/day by 1hr infusion for two consecutive days resulted in peak blood concentrations ranging between 6.2 and 10.2 μM [35]. Although CPA doses used in the metronomic scheme for mice are lower, CPA bioactivation rates about 50-fold higher compared to humans have to be considered [36].

In line with previous studies, acrolein-modified proteins were detected distant to the place of activation [14] also indicating relevant systemic concentrations of acrolein within CPA tumour therapy. Tumour regions accessible *via* blood stream can therefore be reached not only by the DNA cross-linking agent phosphoramide mustard, but also by acrolein. A second possible pathway of acrolein entering the tumour site is transport *via* the metabolites 3-oxopropylglutatione and S-3-hydroxypropyl N-acetylcysteine [37]. In this context, release of acrolein from different thiol conjugates is possible *via* β-elimination after enzymatic activation [38, 39] and is responsible for side effects in lung and bladder as observed with high dose regimes [37].

The metronomic schedule in this study resulted in significant reduction of tumour growth and functional tumour blood flow as detected by reduced Hoechst 33258 fluorescence in treated tumours, indicating antiangiogenic activity of the used treatment regime [40].

Reduction in proliferation of endothelial cells by treatment with activated CPA was detected *in vitro*. However, decrease in proliferation of HUVEC cells cultured with activated CPA or acrolein alone, respectively, suggests a more predominant role for acrolein in influencing proliferation of primary endothelial cells than previously considered. We also observed differences in sensitivity towards acrolein treatment between HUVEC (human EC), PEC (porcine EC) and murine CT26 tumour cells. This largely depends on differences in cellular acrolein detoxification capacity, which can vary between cell types and species. The detoxification process involves enzymes from the ALDH and AKR family [41, 42], but also interceptive systems like cellular glutathione (GSH) [43].

In tumour blood vessel formation, angiogenic endothelial cells migrate towards the direction of angiogenic stimuli (chemotaxis), followed by differentiation processes. During migration, further proliferation occurs. Experiments described by Browder *et al.* showed antimigrative effects of 4-OH-CPA on primary endothelial cells [5]. However, performing the migration assay in the presence of sublethal doses of acrolein resulted in a dose-dependent inhibition of migration capability in primary endothelial cells. Further on, acrolein was shown to inhibit differentiation of primary endothelial cells in terms of tube formation in the matrigel assay, indicating significant interference with the angiogenic process.

This interference regarding migration and tube formation may be based on interaction of acrolein with the F-actin cytoskeleton of endothelial cells. Actin exhibits several nucleophilic reaction sites and can be targeted by Michael addition [15]. In previous studies, acrolein was shown to react with actin in cell free systems in a dose-dependent manner and led to structural distortions and changes in the polymerization rate [44]. Targeting the F-actin cytoskeleton became a focus of research regarding antiangiogenic strategies [45]. Similar to acrolein several known antiangiogenic compounds like cyclosporin A [46], rosiglitazone [47], endostatin [48], endorepellin [49], erianin [50] and thalidomide [51] show interference with the F-actin cytoskeleton, resulting in reduced migration and inhibition of tube/capillary formation ability of endothelial cells.

Endothelial integrin αvβ3 is another crucial element in migration and capillary formation during angiogenic processes, providing interaction with the extracellular matrix, cell signalling and linkage to the actin cytoskeleton [52]. Inhibition of integrin αvβ3 function has been reported to suppress neovascularization and tumour growth [53]. In the current study, acrolein exerted antiangiogenic activity by disturbing integrin αvβ3 clustering in the filopodia of endothelial cells. However, changes in total expression levels, as analysed by antibody staining followed by Fluorescence Activated Cell Sorting (FACS) analysis, were not observed (data not shown).

Besides a possible direct interference with the F-actin cytoskeleton and integrins, acrolein interacts with intracellular pathways, regulating response and expression profiles of proangiogenic and antiangiogenic cytokines [54] like TSP-1, that in turn effect the endothelial phenotype. NF-κB was identified as an important signalling molecule in integrin αvβ3-mediated endothelial cell survival [20] and linked to the PI3K/Akt pathway, influencing proliferation and differentiation [55]. Inhibition of NF-κB activity led to a non-angiogenic endothelial phenotype, and resulted in decreased tube formation in matrigel assays and cell survival in primary endothelial cells [21]. Thus, the detected modulation of NF-κB activity levels in primary endothelial cells by acrolein further interferes with steps in the angiogenic process regarding endothelial survival and differentiation. As NF-κB activity is redox sensitive the increase in NF-κB activity levels at 30 μm (added acrolein) may result from further GSH depletion representing a stress reaction [56]. The up-regulation at 30 μm acrolein was suppressed in the presence of 15μm PDTC, an

inhibitor of the NF-κB pathway [57] (data not shown). Up-regulation of NF-κB activity levels at 30 μM (added acrolein) can further result from decreased precursor p105 levels, which acts as a suppressor on NF-κB activity [58], and from the changed ratio of p50 to p65 (see Fig 6B). Decrease in p50 leads to a decrease of p50-p50 homodimer formation that acts as a repressor due to the lack of transcriptional activation domains [59], whereas p50-p65 and p65-p65 dimers act as transcription factors for NF-κB-regulated gene expression [58].

Acrolein induced TSP-1 expression in endothelial cells may be crucial to mediate a quiescent endothelial phenotype. In several studies, TSP-1 was described as a potent inhibitor of angiogenesis influencing endothelial cell survival [60] and migration [61]; TSP-1 also interferes with integrin signalling [62]. In our study, TSP-1 expression was found to be highly up-regulated in HUVEC cells already at lower concentrations of active acrolein (1.7 μM), as it was detected in blood of patients receiving 60 mg/kg CPA on two consecutive days (up to 10.2 μM) [35]. High concentrations of acrolein (30 μm) increased NF-κB activity and decreased TSP-1 expression levels linking NF-κB activity inversely to TSP-1 expression. However, the interaction between TSP-1 and NF-κB may be mediated *via* Akt, as it was recently shown that increased TSP-1 expression in endothelial cells is linked to a down-regulation of the PI3K/Akt pathway [55] and a bidirectional crosstalk between the NF-κB pathway and Akt exists [63, 64].

In summary, metronomic CPA treatment resulted in decreased tumour progression and reduced blood supply in subcutaneous CT26 tumours. Acrolein adducts in tumour and in tumour endothelial cells indicate a pharmacological role of this metabolite *in vivo*. *In vitro*, acrolein inhibited important key steps in the angiogenic process by disturbing clustering of integrin αvβ3 receptors on the sites of focal adhesions and disturbance of the F-actin cytoskeleton. Further on, acrolein modulated NF-κB signal transduction pathways and influenced TSP-1 expression levels in primary endothelial cells. As a result of this multi-factorial interaction, acrolein inhibited proliferation, migration and tube formation of primary endothelial cells. Our present findings indicate a direct and indirect interaction of acrolein with endothelial cells and resulting interference with the process of tumour progression and angiogenesis, suggesting a critical role for acrolein in metronomically scheduled CPA treatment regimes.

Acknowledgements

We thank Prof Carsten Culmsee for helpful discussions and Dr. Jaroslav Pelisek for providing PEC cells. Miriam Höhn is gratefully acknowledged for excellent technical assistance. These studies were supported by research grants from the Wilhelm Sander Stiftung and the Dr. Mildred Scheel Stiftung.

Reference

1. **Kozekov ID, Nechev LV, Moseley MS, Harris CM, Rizzo CJ, Stone MP, Harris TM.** DNA interchain cross-links formed by acrolein and crotonaldehyde. *J Am Chem Soc.* 2003; 125: 50–61.
2. **Seiner DR, Labutti JN, Gates KS.** Kinetics and Mechanism of Protein Tyrosine Phosphatase 1B Inactivation by Acrolein. *Chem Res Toxicol.* 2007; 20: 1315–20.
3. **Wrabetz E, Peter G, Hohorst HJ.** Does acrolein contribute to the cytotoxicity of cyclophosphamide? *J Cancer Res Clin Oncol.* 1980; 98: 119–26.
4. **Munoz R, Shaked Y, Bertolini F, Emmenegger U, Man S, Kerbel RS.** Anti-angiogenic treatment of breast cancer using metronomic low-dose chemotherapy. *Breast.* 2005; 14: 466–79.
5. **Browder T, Butterfield CE, Kraling BM, Shi B, Marshall B, O'Reilly MS, Folkman J.** Antiangiogenic scheduling of chemotherapy improves efficacy against experimental drug-resistant cancer. *Cancer Res.* 2000; 60: 1878–86.
6. **Emmenegger U, Morton GC, Francia G, Shaked Y, Franco M, Weinerman A, Man S, Kerbel RS.** Low-dose metronomic daily cyclophosphamide and weekly tirapazamine: a well-tolerated combination regimen with enhanced efficacy that exploits tumor hypoxia. *Cancer Res.* 2006; 66: 1664–74.
7. **Zhao D, Jiang L, Hahn EW, Mason RP.** Continuous low-dose (metronomic) chemotherapy on rat prostate tumors evaluated using MRI *in vivo* and comparison with histology. *Neoplasia.* 2005; 7: 678–87.
8. **Damber JE, Vallbo C, Albertsson P, Lennernas B, Norrby K.** The anti-tumour effect of low-dose continuous chemotherapy may partly be mediated by thrombospondin. *Cancer Chemother Pharmacol.* 2006; 58: 354–60.
9. **Ng SS, Figg WD.** Upregulation of endogenous angiogenesis inhibitors: a mechanism of action of metronomic chemotherapy. *Cancer Biol Ther.* 2004; 3: 1212–3.
10. **Armstrong LC, Bornstein P.** Thrombospondins 1 and 2 function as inhibitors of angiogenesis. *Matrix Biol.* 2003; 22: 63–71.
11. **Guo N, Krutzsch HC, Inman JK, Roberts DD.** Thrombospondin 1 and type I repeat peptides of thrombospondin 1 specifically induce apoptosis of endothelial cells. *Cancer Res.* 1997; 57: 1735–42.
12. **DeLeve LD.** Cellular target of cyclophophamide toxicity in the murine liver: role of glutathione and site of metabolic activation. *Hepatology.* 1996; 24: 830–7.
13. **Kachel DL, Martin WJ.** Cyclophosphamide-induced lung toxicity: mechanism of endothelial cell injury. *J Pharmacol Exp Ther.* 1994; 268: 42–6.
14. **Arikketh D, Niranjali S, Devaraj H.** Detection of acrolein-lysine adducts in plasma low-density lipoprotein and in aorta of cyclophosphamide-administered rats. *Arch Toxicol.* 2004; 78: 397–401.
15. **Aldini G, Dalle-Donne I, Vistoli G, Maffei FR, Carini M.** Covalent modification of actin by 4-hydroxy-trans-2-nonenal (HNE): LC-ESI-MS/MS evidence for Cys374 Michael adduction. *J Mass Spectrom.* 2005; 40: 946–54.
16. **Poggi P, Rota MT, Boratto R.** The volatile fraction of cigarette smoke induces alterations in the human gingival fibroblast

cytoskeleton. *J Periodontal Res.* 2002; 37: 230–5.

17. **Horton ND, Biswal SS, Corrigan LL, Bratta J, Kehrer JP.** Acrolein causes inhibitor kappaB-independent decreases in nuclear factor kappaB activation in human lung adenocarcinoma (A549) cells. *J Biol Chem.* 1999; 274: 9200–6.
18. **Valacchi G, Pagnin E, Phung A, Nardini M, Schock BC, Cross CE, van d, V.** Inhibition of NFkappaB activation and IL-8 expression in human bronchial epithelial cells by acrolein. *Antioxid Redox Signal.* 2005; 7: 25–31.
19. **Lambert C, Li J, Jonscher K, Yang TC, Reigan P, Quintana M, Harvey J, Freed BM.** Acrolein inhibits cytokine gene expression by alkylating cysteine and arginine residues in the NF-kappaB1 DNA binding domain. *J Biol Chem.* 2007; 282: 19666–75.
20. **Scatena M, Almeida M, Chaisson ML, Fausto N, Nicosia RF, Giachelli CM.** NF-kappaB mediates alphavbeta3 integrin-induced endothelial cell survival. *J Cell Biol.* 1998; 141: 1083–93.
21. **Patel S, Leal AD, Gorski DH.** The homeobox gene Gax inhibits angiogenesis through inhibition of nuclear factor-kappaB-dependent endothelial cell gene expression. *Cancer Res.* 2005; 65: 1414–24.
22. **Kim JB, Stein R, O'Hare MJ.** Tumour-stromal interactions in breast cancer: the role of stroma in tumourigenesis. *Tumour Biol.* 2005; 26: 173–85.
23. **Brissault B, Leborgne C, Guis C, Danos O, Cheradame H, Kichler A.** Linear topology confers *in vivo* gene transfer activity to polyethylenimines. *Bioconjug Chem.* 2006; 17: 759–65.
24. **Plank C, Zatloukal K, Cotten M, Mechtler K, Wagner E.** Gene transfer into hepatocytes using asialoglycoprotein receptor mediated endocytosis of DNA complexed with an artificial tetra-antennary galactose ligand. *Bioconjug Chem.* 1992; 3: 533–9.
25. **Pelisek J, Engelmann MG, Golda A, Fuchs A, Armeanu S, Shimizu M, Mekkaoui C, Rolland PH, Nikol S.** Optimization of nonviral transfection: variables influencing liposome-mediated gene transfer in proliferating vs. quiescent cells in culture and *in vivo* using a porcine restenosis model. *J Mol Med.* 2002; 80: 724–36.
26. **Baumann F, Schmidt R, Teichert J, Preiss R.** Influence of protein binding on acrolein turnover *in vitro* by oxazaphosphorines and liver microsomes. *J Clin Lab Anal.* 2005; 19: 103–9.
27. **von Gersdorff K, Sanders NN, Vandenbroucke R, De Smedt SC, Wagner E, Ogris M.** The internalization route resulting in successful gene expression depends on both cell line and polyethylenimine polyplex type. *Mol Ther.* 2006; 14: 745–53.
28. **Culmsee C, Zhu C, Landshamer S, Becattini B, Wagner E, Pellecchia M, Blomgren K, Plesnila N.** Apoptosis-inducing factor triggered by poly(ADP-ribose) polymerase and Bid mediates neuronal cell death after oxygen-glucose deprivation and focal cerebral ischemia. *J Neurosci.* 2005; 25: 10262–72.
29. **Gunther M, Waxman DJ, Wagner E, Ogris M.** Effects of hypoxia and limited diffusion in tumor cell microenvironment on bystander effect of P450 prodrug therapy. *Cancer Gene Ther.* 2006; 13: 771–9.
30. **Jeffes EW, Zhang JG, Hoa N, Petkar A, Delgado C, Chong S, Obenaus A, Sanchez R, Khalaghizadeh S, Khomenko T, Knight BA, Alipanah R, Nguyen TV, Shah C, Vohra S, Zhuang JL, Liu J, Wepsic HT, Jadus MR.** Antiangiogenic drugs synergize with a membrane macrophage colony-stimulating factor-based tumor vaccine to therapeutically treat rats with an established malignant intracranial glioma. *J Immunol.* 2005; 174: 2533–43.
31. **von Gersdorff K, Ogris M, Wagner E.** Cryoconserved shielded and EGF receptor targeted DNA polyplexes: cellular mechanisms. *Eur J Pharm Biopharm.* 2005; 60: 279–85.
32. **Hales BF.** Comparison of the mutagenicity and teratogenicity of cyclophosphamide and its active metabolites, 4-hydroxycyclophosphamide, phosphoramide mustard, and acrolein. *Cancer Res.* 1982; 42: 3016–21.
33. **Zhang J, Tian Q, Yung CS, Chuen LS, Zhou S, Duan W, Zhu YZ.** Metabolism and transport of oxazaphosphorines and the clinical implications. *Drug Metab Rev.* 2005; 37: 611–703.
34. **Pass GJ, Carrie D, Boylan M, Lorimore S, Wright E, Houston B, Henderson CJ, Wolf CR.** Role of hepatic cytochrome p450s in the pharmacokinetics and toxicity of cyclophosphamide: studies with the hepatic cytochrome p450 reductase null mouse. *Cancer Res.* 2005; 65: 4211–7.
35. **Ren S, Kalhorn TF, Slattery JT.** Inhibition of human aldehyde dehydrogenase 1 by the 4-hydroxycyclophosphamide degradation product acrolein. *Drug Metab Dispos.* 1999; 27: 133–7.
36. **Wagner T, Heydrich D, Voelcker G, Hohorst HJ.** Blood level and urinary excretion of activated cyclophosphamide and its deactivation products in man. *J Cancer Res Clin Oncol.* 1980; 96: 79–92.
37. **Ramu K, Perry CS, Ahmed T, Pakenham G, Kehrer JP.** Studies on the basis for the toxicity of acrolein mercapturates. *Toxicol Appl Pharmacol.* 1996; 140: 487–98.
38. **Hashmi M, Vamvakas S, Anders MW.** Bioactivation mechanism of S-(3-oxopropyl)-N-acetyl-L-cysteine, the mercapturic acid of acrolein. *Chem Res Toxicol.* 1992; 5: 360–5.
39. **Horvath JJ, Witmer CM, Witz G.** Nephrotoxicity of the 1:1 acrolein-glutathione adduct in the rat. *Toxicol Appl Pharmacol.* 1992; 117: 200–7.
40. **Goertz DE, Yu JL, Kerbel RS, Burns PN, Foster FS.** High-frequency Doppler ultrasound monitors the effects of antivascular therapy on tumor blood flow. *Cancer Res.* 2002; 62: 6371–5.
41. **Bunting KD, Townsend AJ.** Dependence of aldehyde dehydrogenase-mediated oxazaphosphorine resistance on soluble thiols: importance of thiol interactions with the secondary metabolite acrolein. *Biochem Pharmacol.* 1998; 56: 31–9.
42. **Gardner R, Kazi S, Ellis EM.** Detoxication of the environmental pollutant acrolein by a rat liver aldo-keto reductase. *Toxicol Lett.* 2004; 148: 65–72.
43. **Wlodek L.** The reaction of sulfhydryl groups with carbonyl compounds. *Acta Biochim Pol.* 1988; 35: 307–17.
44. **Dalle-Donne I, Carini M, Vistoli G, Gamberoni L, Giustarini D, Colombo R, Maffei FR, Rossi R, Milzani A, Aldini G.** Actin Cys374 as a nucleophilic target of alpha,beta-unsaturated aldehydes. *Free Radic Biol Med.* 2007; 42: 583–98.
45. **Giganti A, Friederich E.** The actin cytoskeleton as a therapeutic target: state of the art and future directions. *Prog Cell Cycle Res.* 2003; 5: 511–25.
46. **Rafiee P, Heidemann J, Ogawa H, Johnson NA, Fisher PJ, Li MS, Otterson MF, Johnson CP, Binion DG.** Cyclosporin A differentially inhibits multiple steps in VEGF induced angiogenesis in human microvascular endothelial cells through altered intracellular signaling. *Cell Commun Signal.* 2004; 2: 3.
47. **Sheu WH, Ou HC, Chou FP, Lin TM, Yang CH.** Rosiglitazone inhibits endothelial proliferation and angiogenesis. *Life Sci.* 2006; 78: 1520–8.

48. **Skovseth DK, Veuger MJ, Sorensen DR, De Angelis PM, Haraldsen G.** Endostatin dramatically inhibits endothelial cell migration, vascular morphogenesis, and perivascular cell recruitment *in vivo*. *Blood.* 2005; 105: 1044–51.
49. **Bix G, Fu J, Gonzalez EM, Macro L, Barker A, Campbell S, Zutter MM, Santoro SA, Kim JK, Hook M, Reed CC, Iozzo RV.** Endorepellin causes endothelial cell disassembly of actin cytoskeleton and focal adhesions through alpha2beta1 integrin. *J Cell Biol.* 2004; 166: 97–109.
50. **Gong YQ, Fan Y, Wu DZ, Yang H, Hu ZB, Wang ZT.** *in vivo* and *in vitro* evaluation of erianin, a novel anti-angiogenic agent. *Eur J Cancer.* 2004; 40: 1554–65.
51. **Tamilarasan KP, Kolluru GK, Rajaram M, Indhumathy M, Saranya R, Chatterjee S.** Thalidomide attenuates nitric oxide mediated angiogenesis by blocking migration of endothelial cells. *BMC Cell Biol.* 2006; 7: 17.
52. **Mi J, Zhang X, Giangrande PH, McNamara JO, Nimjee SM, Sarraf-Yazdi S, Sullenger BA, Clary BM.** Targeted inhibition of alphavbeta3 integrin with an RNA aptamer impairs endothelial cell growth and survival. *Biochem Biophys Res Commun.* 2005; 338: 956–63.
53. **Cai W, Chen X.** Anti-angiogenic cancer therapy based on integrin alphavbeta3 antagonism. *Anticancer Agents Med Chem.* 2006; 6: 407–28.
54. **Kehrer JP, Biswal SS.** The molecular effects of acrolein. *Toxicol Sci.* 2000; 57: 6–15.
55. **Bussolati B, Assenzio B, Deregibus MC, Camussi G.** The proangiogenic phenotype of human tumor-derived endothelial cells depends on thrombospondin-1 downregulation *via* phosphatidylinositol 3-kinase/Akt pathway. *J Mol Med.* 2006; 84: 852–63.
56. **Filomeni G, Aquilano K, Rotilio G, Ciriolo MR.** Antiapoptotic response to induced GSH depletion: involvement of heat shock proteins and NF-kappaB activation. *Antioxid Redox Signal.* 2005; 7: 446–55.
57. **Schreck R, Meier B, Mannel DN, Droge W, Baeuerle PA.** Dithiocarbamates as potent inhibitors of nuclear factor kappa B activation in intact cells. *J Exp Med.* 1992; 175: 1181–94.
58. **Chen ZJ.** Ubiquitin signalling in the NF-kappaB pathway. *Nat Cell Biol.* 2005; 7: 758–65.
59. **Tong X, Yin L, Washington R, Rosenberg DW, Giardina C.** The p50-p50 NF-kappaB complex as a stimulus-specific repressor of gene activation. *Mol Cell Biochem.* 2004; 265: 171–83.
60. **Jimenez B, Volpert OV, Crawford SE, Febbraio M, Silverstein RL, Bouck N.** Signals leading to apoptosis-dependent inhibition of neovascularization by thrombospondin-1. *Nat Med.* 2000; 6: 41–8.
61. **Dawson DW, Pearce SF, Zhong R, Silverstein RL, Frazier WA, Bouck NP.** CD36 mediates the *In vitro* inhibitory effects of thrombospondin-1 on endothelial cells. *J Cell Biol.* 1997; 138: 707–17.
62. **Sund M, Hamano Y, Sugimoto H, Sudhakar A, Soubasakos M, Yerramalla U, Benjamin LE, Lawler J, Kieran M, Shah A, Kalluri R.** Function of endogenous inhibitors of angiogenesis as endothelium-specific tumor suppressors. *Proc Natl Acad Sci USA.* 2005; 102: 2934–9.
63. **Meng F, Liu L, Chin PC, D'Mello SR.** Akt is a downstream target of NF-kappa B. *J Biol Chem.* 2002; 277: 29674–80.
64. **Meng F, D'Mello SR.** NF-kappaB stimulates Akt phosphorylation and gene expression by distinct signaling mechanisms. *Biochim Biophys Acta.* 2003; 1630: 35–40.